Engineering Structures 236 (2021) 112138

Contents lists available at ScienceDirect

Engineering Structures

journal homepage: www.elsevier.com/locate/engstruct

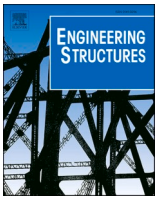

Rotation capacity of corroded RC beams with special ductility tempcore rebars

José Santos [a,c,*], António Abel Henriques [b,c]

[a] UMa - University of Madeira, FCEE - Faculty of Exact Sciences and Engineering, DECG - Department of Civil Engineering and Geology, 9020-105 Funchal, Portugal
[b] University of Porto, Faculty of Engineering, Department of Civil Engineering, 4200-465 Porto, Portugal
[c] CONSTRUCT-LABEST, Faculty of Engineering (FEUP), University of Porto, Portugal

ARTICLE INFO

Keywords:
Corrosion
Damage
Eurocode 2
Experimental campaign
Numerical modelling
Reinforced concrete
Ultimate deflection
Ultimate load

ABSTRACT

The corrosion of reinforced concrete structures influences not only their structural strength but also their ductility. In this scenario, the use of Special Ductility Tempcore rebars, which belong to the highest ductility class, can reduce the risk of having a brittle failure when corrosion occurs.

Therefore, this paper presents experimental and numerical studies to evaluate the rotation capacity of corroded RC beams with this type of steel. The experimental part consists of testing five beams to rupture and the numerical part uses the non-linear finite element method to correctly model the beam's behaviour.

The results indicate that for 20% damage, the rotation capacity reduced about 50%; however, these values are still higher than the Eurocode 2 normalized curve. In this scenario, the ultimate load only reduces 12%. Nevertheless, corrosion affects the ultimate deflection of isostatic beams much more than hyperstatic beams.

1. Introduction

The European construction market is worth about 1.6 billion euro. Activities concerning the evaluation, repair and restoration of concrete structures are estimated as 35% of all the work in the building sector. The main reason for the degradation of reinforced concrete (RC) structures is the corrosion of steel reinforcement [1]. In literature, the corrosion of rebars is usually divided into two types, pitting and general corrosion.

The mechanical consequences of corrosion are: i) reduction in the cross-sectional area of the rebars, ii) deterioration of the bond with the surrounding concrete and iii) loss of concrete cover [2]. This means that, besides the structural strength being reduced, the ductility of reinforced concrete structures is also severely reduced by rebars' corrosion.

The ductility of reinforced concrete elements is an essential property to accommodate the change that occurs in a deformation field during its service lifetime [3], especially when high redistribution of bending moments was applied [4]. The ductility can be evaluated at several levels: material, section and structural. In this paper, the last is mainly applied. There are several studies concerning the influence of corrosion on ductility, with the study of corroded rebars and corroded RC beams being most relevant for this paper, as detailed below.

Regarding corroded rebars, Du et al. [5] states that the ultimate strain of corroded reinforcement reduces much more significantly than their yield and ultimate strengths. Similarly, François et al. [6] concluded that a reduction of the ultimate strain appeared to be the major effect of corrosion, which could affect compliance with standards. Moreover, Tang et al. [7] noticed that both the yield and ultimate strength linearly decreased with an increase of corrosion loss while the elongation and ductility decreased exponentially. Zhu et al. [8] noted that the residual cross-section shape and the amount of cross-section loss had considerable influence on the ductility of bars. Likewise, Imperatore et al. [9] observed that pitting corrosion provokes a higher decrease in ultimate strain, yield and ultimate strength. Chen et al. [10] observed that when the corrosion level exceeded a critical value, the region outside the pit did not develop yielding, which means that rebar ductility decreases a lot. Hawileh et al. [11] observed that the yield and tensile strength decreased 26% and the ultimate strain reduced 76.6%, for corrosion damage level of 19.6%. Andisheh et al. [12] reports that the reductions of mechanical properties related in literature has a large scatter and the use of reduction factors could not be safe.

Concerning corroded RC beams, Castel et al. [13] noticed that in service a reduction of bending stiffness was observed due to degradation in the tensile zone and for ultimate behaviour the loss of steel cross-

* Corresponding author.
E-mail address: jmmns@fe.up.pt (J. Santos).

https://doi.org/10.1016/j.engstruct.2021.112138
Received 27 July 2020; Received in revised form 12 February 2021; Accepted 26 February 2021
Available online 27 March 2021

section leads to a reduction of bearing capacity and ductility. Dang & François [14,15] found that the reduction of ductility in bending behaviour was more pronounced on the reduction of load-bearing capacity. Almusallam et al. [16] concluded that the ultimate deflection decreases with an increase in the magnitude of reinforcement corrosion, leading to a marked and progressive reduction in the ductility. Ou & Nguyen [17], found that as the corrosion level in tension reinforcement increased, the failure mode of the beam changed from flexural shear due to crushing of core concrete to flexural tension due to fracture of tension reinforcement, and corrosion had a significant negative effect on the yield drift, yield load, peak load and ultimate drift. Yadav et al. [18] concluded that an increase in the corrosion percentage of reinforcement bars from 10 to 30% decreased the plastic hinge length, making it undesirable as a seismic member. Ye et al. [19] found that neither the average mass loss ratio of corroded rebar nor the crack widths can be a reliable way to estimate the residual capacity of beams. However, Dasar et al. [20] established good correlations between crack width and cross-section loss and between cross-section loss and ultimate capacity loss. Azad et al. [21] states that size-effect of the tension bars should be taken into account in the calculation of the flexural capacity of a corroded concrete beam.

In corroded RC beams, Yu et al. [22] found that 1% reduction in cross-section corresponds to 1% reduction in yielding and ultimate capacity, and that the influence of corrosion on the ductility of RC beams depends on the initial ductility of the steel bar. Similarly, Hansapinyo et al. [23] concluded that the ultimate strength decreased linearly with the amount of corrosion and the ductility also decreased with the increase of the corrosion.

In corroded RC beams, Du et al. [24] noted that the combined effect of loading and corrosion impairs beam strength and ductility more significantly. Likewise, Liu et al. [25] noted that strength and ductility are significantly impaired due to the simultaneous effect of loading and corrosion. Dong et al. [20] also concluded that simultaneous loading and corrosion led to more severe and faster cracking damage on the beams and reduced the beams' ductility. Similarly, the coupled action of corrosion and fatigue increases the structural deterioration, reducing the service lifetime of RC structures [26], because accelerates the fatigue crack propagation [27]. In this scenario, the yield and ultimate strength of rebars decrease, and the yield plateau is shortened or even disappeared, which motivates the development of a new constitutive relationship for the mechanical behaviour of rebars after fatigue [28].

Concerning the numerical simulation of corroded RC beams, several researchers performed their studies, as described below. Lundgren [29] noted that corrosion can increase the bond capacity of smooth bars to about the level of ribbed bars, however high corrosion levels may damage the bond, especially if transverse reinforcement is not supplied. Sæther & Sand [30] successfully simulated the mechanical behaviour of reinforced concrete members with corroded steel bars. Biondini & Vergani [31] stated that designing concrete structures exposed to corrosion for durability needs to rely on structural analysis methods capable of accounting for the global effects of local damage phenomena on the overall system performance. According to Hanjari et al. [32], not considering pitting corrosion can lead to an overestimation of structural strength; therefore, both general corrosion and pitting corrosion should be taken into account in modelling corroded concrete structures. Stewart [33] also indicates that the inclusion of accurate mechanical properties of corroded rebars in numerical models is essential to achieve good results, especially to evaluate the reliability and to estimate the lifetime of structures. Devi et al. [34] found that the reduction of the cross-sectional area and yield strength is the best technique to simulate the behaviour of rebars when modelling RC corroded beams. Kallias & Rafiq [35] numerically found the reasons for the large scatter observed during the laboratory tests of corroded RC beams.

As described above, several studies tried to quantify the ductility of corroded RC beams; however, few of them have been dedicated to specifically evaluate the rotation capacity, although in most of them this could be estimated from their results. Note that in literature, the most relevant models to calculate the rotation capacity of non-corroded RC beams include the Stuttgart model, Naples model, Darmstadt-Leipzig model, Zürich model, Delft model (all detailed in [3]), Coimbra model [36], Adelaide model [37] and Hong Kong model [38].

Moreover, the variety of steels used is representative of several ages and places of production; the final results are dependent on the initial steel properties [22], which increase the scattering of results. The production of rebars has changed over the years. Although Tempcore rebars have been used for 50 years, in 2003 a new enhanced generation of Tempcore rebars was created [39], called Special Ductility Weldable Steel. This was developed to be used in seismic regions, where high levels of ductility are required. The main differences to the previous rebars are: i) satisfies the rigorous ductility requirements of Model Code 2010 [40] (class D) and Eurocode 2 [41] (class C), namely: maximum values of $k'=f_{y,actual}/f_{y,nominal}$, minimum and maximum characteristic values of $k=(f_t/f_y)_k$, the minimum characteristic value of strain at maximum force (ε_{uk}), bendability and bond characteristics, ii) weldability, and iii) minimum number of cycles (tensile and compression) without breaking.

The internal mechanical properties of these rebars (with and without damage) is detailed in [42], where is shown that when local damage is introduced in rebar, the main anomaly is the decrease of the ultimate strain since the yield strength reduction is partially offset by the steel hardening. Thus, the rotation capacity of beams with these new rebars in case of corrosion is unknown but relevant to allow estimating the strength and ductility of new structures when corroded in future.

This paper presents experimental and numerical studies to evaluate the rotation capacity of corroded RC beams with Special Ductility Tempcore rebars. Two levels and two combinations of corrosion were applied in simple supported beams. Pitting corrosion was simulated by introducing local damage in the rebars, while general corrosion was simulated by reducing the bond between rebar and concrete. Numerical simulation was also done, initially to evaluate if the numerical models can rigorously predict the rotation capacity of corroded beams and, in the end, to make an additional study with continuous beams where the ductility of rebars is even more relevant.

2. Experimental work

To quantify the rotation capacity in reinforced concrete beams with corroded Special Ductility rebars, an experimental campaign was developed. Five simple supported beams with a tensile reinforcement ratio of 0.6% and different damage levels were tested to rupture. These beams had a length of 2.9 m (2.7 m free span), a width of 0.30 m and a height of 0.35 m (Fig. 1). In these beams, the tension reinforcement was 3ϕ16 (3 rebars of 16 mm diameter), the compression reinforcement was 2ϕ6 (2 rebars of 6 mm diameter for constructive reasons) and the shear reinforcement was ϕ8//0.20 (closed stirrups of 8 mm diameter spaced by 0.20 m). The concrete cover of stirrups was 20 mm. In general, rotation capacity may be limited by either reinforcement ductility or by limiting concrete compression strain. With the selected value of tensile reinforcement ratio, it is expected to achieve nearly the maximum rotation capacity, which coincides with the transition between the types of failure. So, it is expected that for the undamaged beam, failure is due to concrete in compression and for the four damaged beams, the failure is due to lack of reinforcement ductility.

In this work the damage on Tempcore rebars was induced in an artificial way to simulate two types of corrosion: a) reduction of cross-sectional area (Fig. 2a), like pitting corrosion, and b) add to this a reduction of bonding using an insulating tape (thickness 0.11 mm) on the rebar surface (Fig. 2b), like simultaneous general and pitting corrosion.

Table 1 shows the type of damage and its intensity for each beam. The values indicated for pitting damage correspond to the maximum reduction of cross-section area (with a semi-circular shape of radius 5

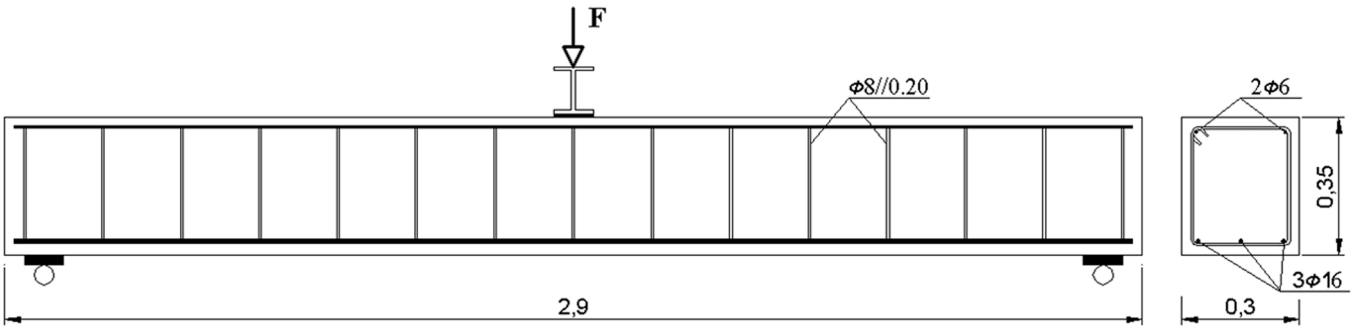

Fig. 1. Beam layout and cross-section [m].

Fig. 2. Artificial damage: a) pitting, b) general.

Table 1
Description of the analysed beams.

Beam	Pitting Damage	General Damage
V1	0%	No
V2	10%	No
V3	20%	No
V4	10%	Yes
V5	20%	Yes

mm (10% damage) and 8 mm (20% damage)) of rebars, with these local damages repeated every 10 cm along and with one exactly at midspan. Note that the semi-circular shape of Fig. 2a is in accordance with experimental results obtained by Liu et al. [43]. The unbonded zone (in beams V4 and V5) was applied along the rebars except near the supports, with the total length (where insulating tape was applied) equal to 2 m.

Note that, in general, pitting corrosion is produced at several points and not only at so localized points of the rebar, as considered here with a uniform spacing of 10 cm. Note also that general corrosion consists of a reduction of cross-section and not only a reduction in bond stress between concrete and rebar, as done here. However, the simplified hypothesis used here are more demanding in terms of strength and ductility than real corrosion, so they are conservative.

The mechanical properties of the materials were: i) concrete: f_c = 34.4 MPa (cylinder compressive strength), f_{ct} = 2.6 MPa (axial tensile strength) and E_c = 24.6 GPa (modulus of elasticity), and ii) rebars: f_y = 537 MPa (yield strength), f_u = 649 MPa (tensile strength), ε_{sh} = 1.4% (strain at the beginning of hardening), ε_u = 10.9% (strain at maximum load), E_s = 193 GPa (modulus of elasticity) and E_{sh} = 3.4 GPa (strain hardening modulus). Fig. 3 shows the force-strain curves for damaged Tempcore rebars. The base length used for strain calculation was 5ϕ and includes one pitting damage.

As the damage is localized, the plastic deformations concentrate in these zones, which leads to a substantial reduction in strain at maximum force (from 10.9% to 6.3% and 5.1%, that is, a reduction of 42 and 53% in this parameter, for damages of 10 and 20%, respectively). Note that in these scenarios (pitting damage of 10 and 20%), the steel is not a ductility class C (Eurocode 2) or D (Model Code 2010) anymore, but as it remains with considerable strain at maximum force, the steel would be classified as ductility class B. The reduction of yield strength was 79% higher than the reduction in cross-sectional area, which is explained by the fact that surface layer of Tempcore rebars is much harder and resistant than the core layer [42]. The reduction of tensile strength was only 28% higher than the reduction in cross-sectional area.

The simple supported beams were vertically loaded at midspan by a hydraulic jack, with a 10 cm loading length through an auxiliary steel beam (Fig. 1 and Fig. 4), while at the ends, free supports were used to allow free horizontal displacements. The tests were carried out in displacement control mode with a loading velocity equal to 0.02 mm/s.

Some LVDTs (linear variable displacement transducers) were used (Fig. 4a): i) one for measuring the vertical displacement of beams at midspan, ii) two in the horizontal position for measuring the elongation of the beams on compression and tension fibres at midspan (placed at 10 mm from the bottom and top with a 60 cm measuring length) to evaluate the rotation, and iii) others not considered in this paper. In the opposite surface (Fig. 4b) from where LVDTs were applied, a mesh of points was plotted on the beams in a rectangular matrix to allow these points to be followed by a video camera during the tests. After that, using a digital image correlation (DIC) routine developed by the authors in Matlab, the positions of each point during the test were calculated. Note that from the horizontal LVDTs or the DIC system, the maximum horizontal strains (compressive and tensile) could be calculated and from this, the relative rotation of the sections could be calculated.

A load cell in the hydraulic jack measured the total load applied to

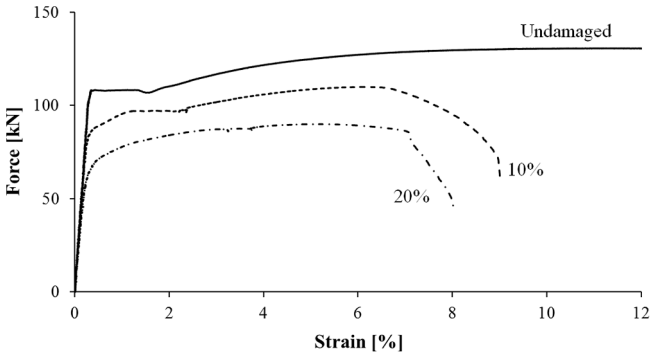

Fig. 3. Force-Strain curves for damaged Tempcore rebars.

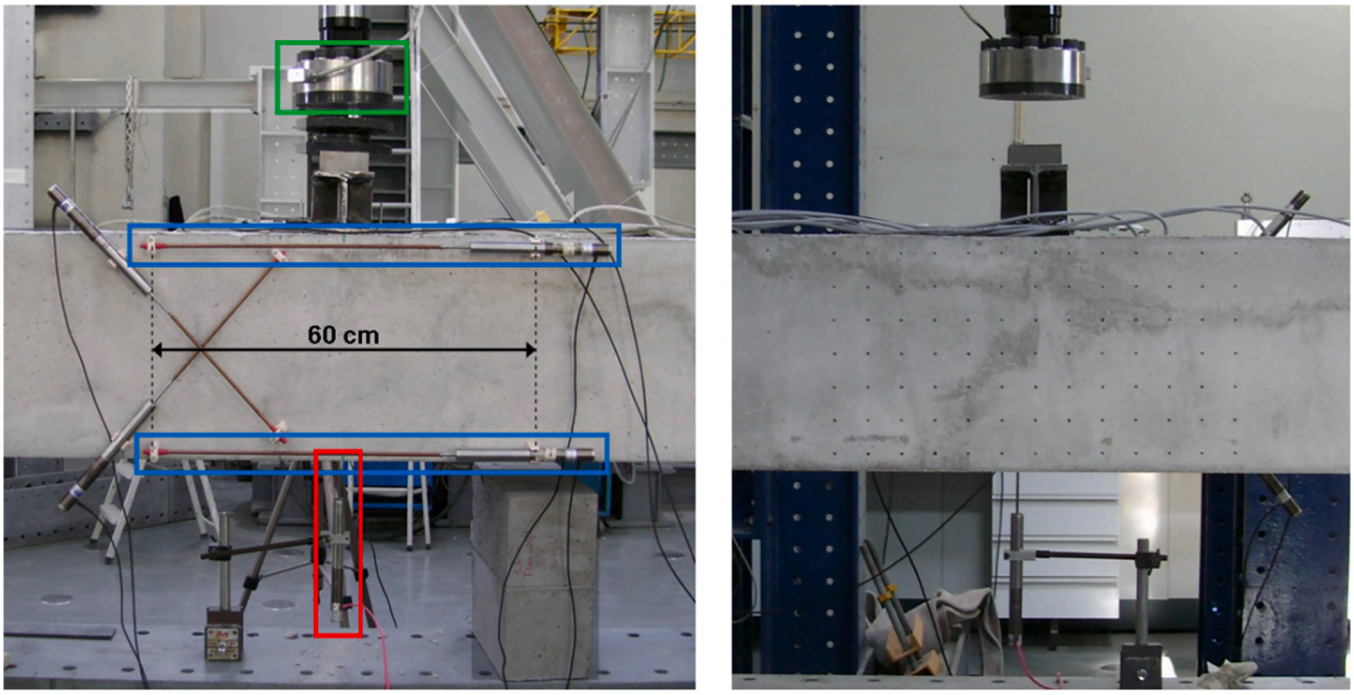

Fig. 4. Beam setup: a) electric sensors, b) mesh of points for DIC system.

the beams. Although not used in this paper, several electrical resistance strain gauges (Vishay, type EP-08-125BT-120) were also glued to the rebars, separated longitudinally by 15 cm and with one at midspan.

3. Numerical simulation

In addition to the experimental work, a numerical simulation was also carried out to evaluate the ability of numerical models to estimate the rotation capacity of reinforced concrete beams with damaged rebars. Note that at the end of Section 6, an additional numerical study with continuous beams was done, but it is not detailed in this section. The beams tested to rupture, as described in the previous section, were simulated using the finite element method with non-linear behaviour of concrete, rebars and bond-slip.

The applied models were developed on Diana software [44] (Fig. 5). Concrete was simulated by regular four-node plane stress elements, with 0.01x0.01 m dimensions and a 2x2 integration scheme (10150 elements). Compression rebars and stirrups were simulated by embedded bar reinforcements (815 elements). More details about the modelling of these beams can be found in [45].

Concerning tension rebars, two distinct implementations were developed for each beam: i) first, rebars were simulated by an embedded bar reinforcement (290 elements), and ii) afterwards, rebars were simulated by truss elements (290 elements) coupled to the bond elements (290 elements) that connected to the concrete mesh (Fig. 6). The bond element was a regular four-node plane stress elements, with dimensions: 0.01x0.001 m and integration scheme 1x1. This bond element, which also takes into account the influence of steel strain on bond, is described in detail in [46]. Several laws for the relationship between bond stress and slip were applied (Proposed [47], MC2010, MC90). Regarding the simulation of the bond reduction due to the insulating tape on the rebar surfaces of beams V4 and V5, a reduction of 50% in the bond stress was assumed.

For concrete elements, the combination of Rankine Principal Stress (in tension) with Drucker–Prager (in compression) was selected for rupture criteria to avoid: i) some incoherencies in mesh deformation after cracking, in the Total Strain Models [44,48], and ii) the unrealistic constant value for shear retention, needed in the Multi-Directional Fixed Crack Model [44,48].

In the elastic range, the properties of concrete were: $E = 24.6$ GPa and $\nu = 0.2$. For non-linear tension behaviour, the following parameters were defined: $f_{ct} = 2.6$ MPa and the Hordijk curve (with $G_f = 138$ N/m) for tension softening. The value of G_f was calculated from f_c using the equation from Model Code 2010 [40].

For non-linear compression behaviour, the Drucker–Prager law (with cohesion: $c = 0.42\, f_c$ and friction and dilatancy angles: $\varphi = \psi = 10°$) for

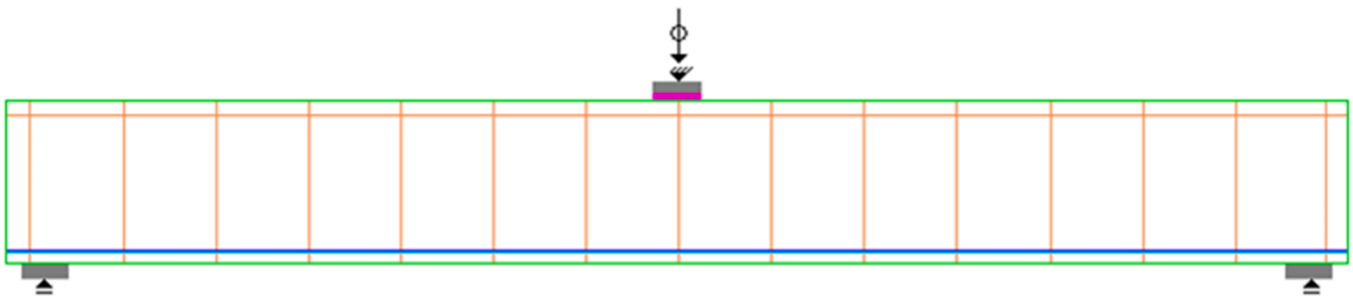

Fig. 5. Major elements of the numerical model.

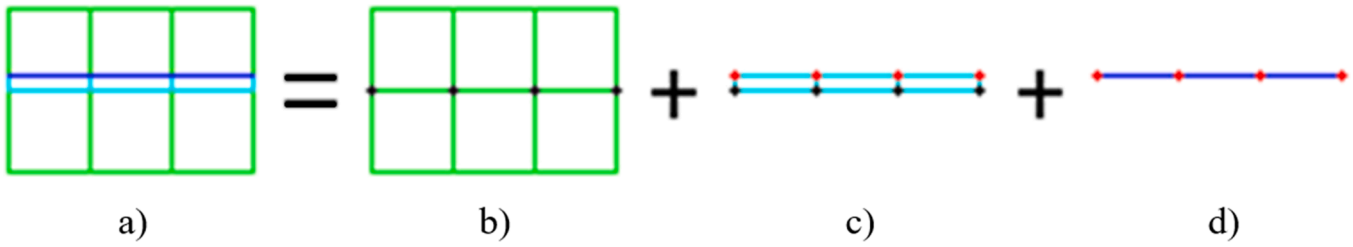

Fig. 6. Detail of the connection between concrete and rebar: a) total mesh, b) concrete mesh, c) interface mesh (bond elements), d) rebar mesh.

isotropic plasticity and a parabolic curve (with $G_C = 25000$ N/m) for strain hardening were chosen. The selected values for plasticity parameters consider the behaviour of concrete under biaxial states of stress [44]. The value for G_C was previously calibrated for compressive rupture.

4. Experimental results

According to Equation (1), the rotation capacity (θ_{pl}) can be estimated by the difference between the total rotation (θ_{tot}) at maximum load level and the rotation at the onset of rebar yielding (θ_y) [3].

$$\theta_{pl} = \theta_{tot} - \theta_y \quad (1)$$

In Fig. 7, the curves of rotation capacity versus rebar damage are shown for the two simulated corrosion formats described in Section 2. The main remark is that rotation capacity is seriously influenced by corrosion. Note that for pitting corrosion damage up to 10%, the rotation capacity was not significantly changed, but for higher values, large reductions occurred in the rotation capacity. Additionally, when general and pitting corrosion act simultaneously, the rotation capacity was always influenced by the damage. For 20% damage, both results were quite similar, with a rotation capacity reduction close to 50%.

The cracking patterns for beams V3 and V5, both with 20% damage, are shown in Fig. 8. For pitting corrosion (Fig. 8a), a very regular pattern with cracks spaced approximately 10 cm was observed, with all cracks equally opened. However, for general and pitting corrosion (Fig. 8b), 20 cm crack spacing was observed, with the two central cracks more opened than the others. These facts were confirmed by the total rotation measurements in Fig. 9, which indicated some curves coincide for general and pitting corrosion (Fig. 9b). In these figures, the base length (Lo) is the length, centred in the middle of the beam, where the total rotation is measured. Note that for pitting corrosion (Fig. 9a), similar increases in total rotation were observed since the base length (Lo) increases, which means that all hinges had similar deformations.

In Fig. 10 the Force-Midspan deflections curves are shown. For pitting corrosion (Fig. 10a), although the damage inserted on rebars was different, the curves are similar in the post-yield range until 50 mm. Otherwise, for simultaneous general and pitting corrosion (Fig. 10b),

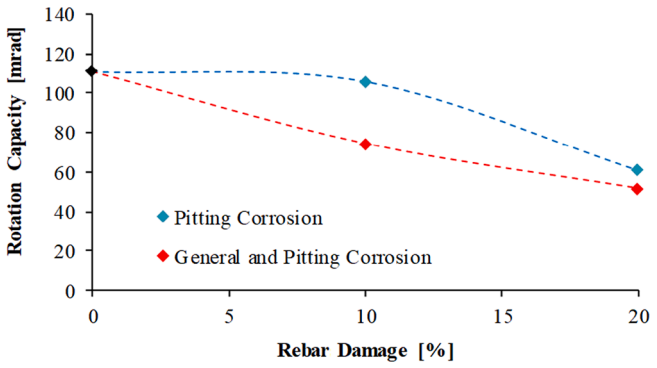

Fig. 7. Rotation capacity as a function of rebar damage.

near failure, the load capacity for each deflection is different, as elucidated in Section 6. For 20% damage, the maximum load for damaged beams was about 152 kN for both beams (V3 and V5), while for the undamaged beam (V1), the maximum load was 172 kN, which means a reduction of 12% in the damaged beams' capacity.

5. Numerical results

The deflection of the structures is a variable easily perceptible. In the tested simple supported beams, the midspan deflection is proportional to the total rotation (θ_{tot}). For this reason, the midspan deflection is used in this section dedicated to the numerical results.

Fig. 11 shows the Force-Midspan deflection curves obtained for beam V2, considering several bond-slip relationships and the experimental result. The curves obtained for the other beams were similar. Notice that all the numerical results were very close to the experimental result.

To evaluate the ability of numerical models in estimating the maximum midspan deflection or the rotation capacity, the relative maximum midspan deflection for all tested beams (maximum deflection numerically calculated divided by maximum deflection measured) is shown in Fig. 12. Despite the very different bond-slip relationships used in the several models, the scattering of the results was not high. Note that the numerical results show higher deflection estimations for simultaneous general and pitting corrosion (V4 and V5) than for pitting corrosion (V2 and V3), as discussed in Section 6.

The numerical crack patterns are exhibited in Fig. 13. These patterns are comparable to the experimental patterns in Fig. 8. For pitting corrosion (Fig. 13a) a very regular pattern with cracks equally spaced by 10 cm was observed. This pattern was also registered in the experimental work. Regarding the general and pitting corrosion (Fig. 13b) the cracks were more distant than in only pitting corrosion (Fig. 13a). Once more, this pattern was slightly similar to the experimental work.

6. Discussion

To evaluate the rotation capacity of corroded RC beams with Special Ductility Tempcore rebars, experimental and numerical studies were realized. One of the limitations of this work is the reduced number of experimental tests. However, one of the most relevant points is the use of a specific type of rebar.

Regarding the experimental tests, the decreasing rotation capacity with corrosion was expected, taking into account that the reduction of cross-section area was done only at localized points. The differences found out between the two types of corrosion for damage up to 10% suggests that the bond between concrete and rebar is very important for the range of moderate damages, but for higher damages, its influence becomes negligible. This suggestion is also sustained in the fact that bond increases for initial corrosion [49–51]. The influence of bond on the ductility of slabs with corroded rebars was also discussed and supported by other authors [52]. When general and pitting corrosion acted simultaneously, the reduction of rotation capacity was 2.5 times higher than for the rebar damage.

In Fig. 14 the results obtained for the rotation capacity of damaged beams are compared with the Eurocode 2 normalized curve for rotation

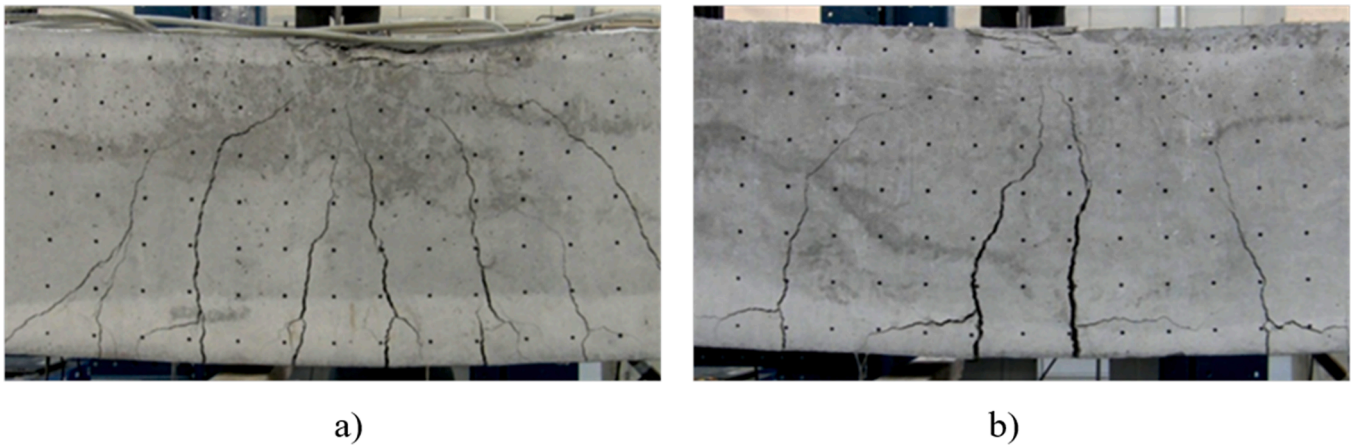

Fig. 8. Cracking patterns near the failure: a) pitting corrosion (V3), b) general and pitting corrosion (V5).

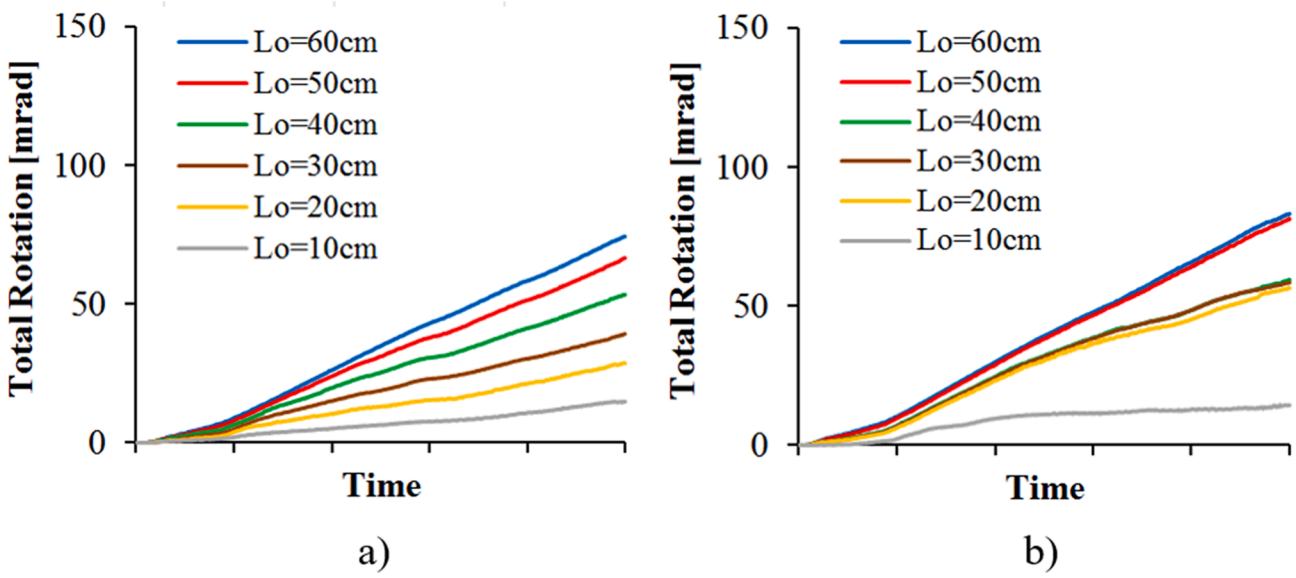

Fig. 9. Total rotation for different base lengths (Lo): a) pitting corrosion (V3), b) general and pitting corrosion (V4).

capacity in undamaged beams. This curve represents the characteristic values of rotation capacity corresponding to the fifth percentile. Despite the high reduction of rotation capacity for damage up to 20%, the values obtained from the tests were always higher than the Eurocode 2 curve.

This fact indicates that even hyperstatic RC structures with corrosion up to 20% can guarantee a level of ductility similar to the implicit ductility design values for an undamaged structure, which allows at least reaching the ultimate design deflection for current structures, that is, having a ductile failure. However, depending on the degree of corrosion, the ultimate design load could not be achieved. Notice that Yu et al. [22] concluded that highly ductile steel bars belonging to Class C according to Eurocode 2 could prevent the brittle collapse of corroded RC beams because of sufficient residual ductility of the corroded steel bars, which is in agreement with these results.

Regarding the maximum load, although 20% damage was introduced, only a 12% reduction in beams capacity was observed. This could be explained by the fact that the steel in the undamaged beam (V1) only achieved the yield strength (failure due to concrete in compression), while the steel in the damaged beams (V3 and V5) achieved the ultimate strength (failure due to reinforcement).

An explanation for the similarities between curves in Fig. 10a, comparing to Fig. 10b, is related to the bond stress. In the first case, the bond stress is high, while in the second case the bond stress is low. Since bond stress is high, the stress in the rebar is high, so more force is reached, for the same beam deflection. Consequently, for the same midspan deflection, since the bond is high, the applied force could be similar even though the levels of corrosion are different.

Concerning to the numerical simulation, the obtained results were in good agreement with the experimental work, especially considering the usual dispersion of the experimental work and the approximations in the formulations of concrete. Though, it was only possible with a rigorous selection of the models for concrete, particularly in compression. The different relationships for bond-slip moderately influenced the results, particularly near the rupture. As a matter of fact, in service, all the relationships are similar.

The results of numerical simulations (Fig. 12) allow emphasising the importance of bond-slip modelling in estimating the ductility of RC elements with corroded rebars. It should also be mentioned that the model proposed by authors [47] tends to achieve better results. The higher values of numerical midspan deflection for general and pitting corrosion obtained in Fig. 12 could be explained by the inadequate selection of the bond-slip relationship (reduction of 50% in the bond stress) when general corrosion is also present.

The experimental and numerical crack patterns are similar. In fact, the location of cracks (Fig. 8 and Fig. 13) coincides with the positions of local damage introduced in the rebars, which was previously defined as

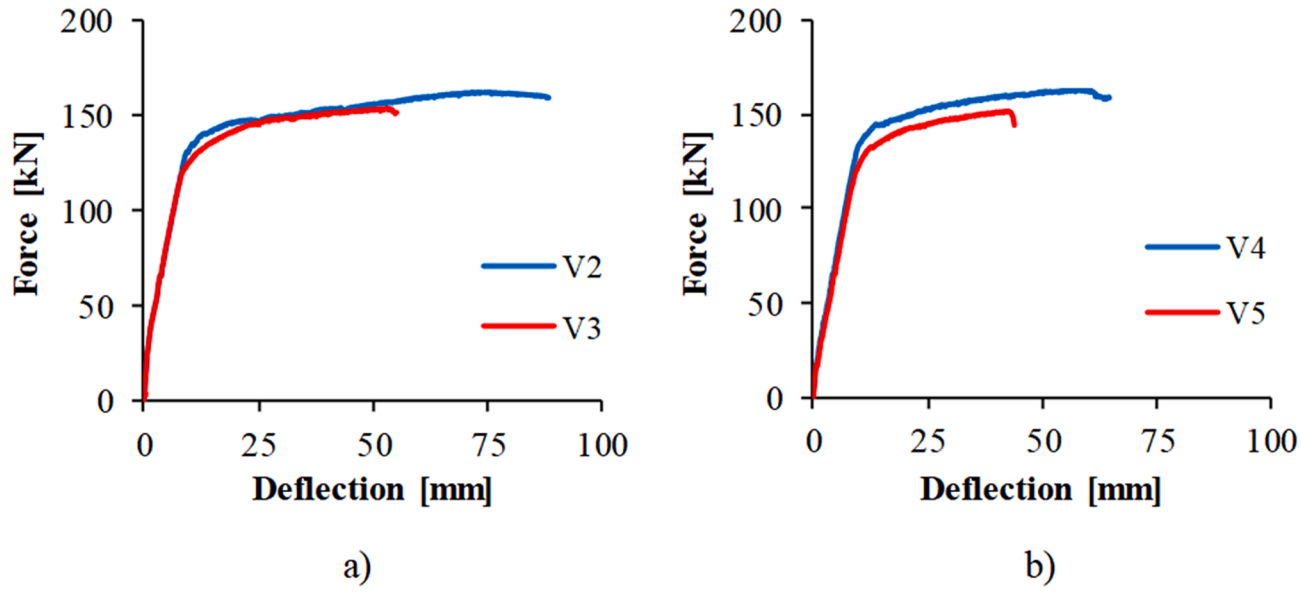

Fig. 10. Force-Midspan deflection curves: a) pitting corrosion, b) general and pitting corrosion.

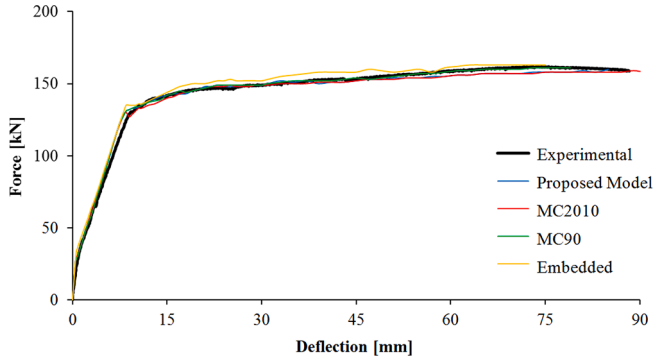

Fig. 11. Force vs Midspan deflection for beam V2 (plots for experimental and numerical simulations).

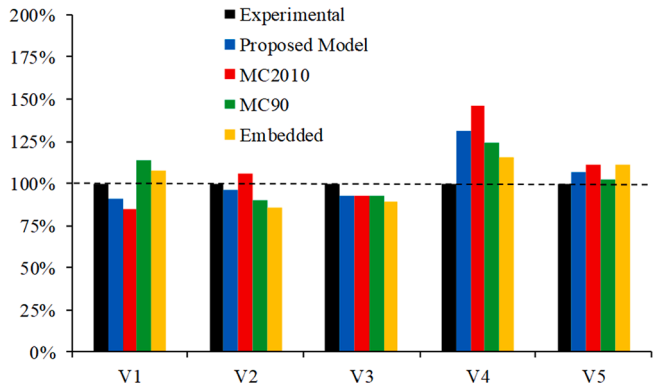

Fig. 12. Relative maximum midspan deflection.

equally spaced by 10 cm. This regular pattern could be one of the reasons why rotation capacity remains higher than the Eurocode 2 normalized curve, although local damage reached 20%. This conclusion could also be useful for situations where, in general, high rotation capacity is required. If previous local damage is introduced in concrete to create a crack pattern with many cracks, high values of rotation capacity would probably be achieved.

With numerical models giving reliable results, an additional numerical analysis was done to evaluate the relevance of having high ductile rebars when corrosion occurs in hyperstatic beams. Thus, a continuous beam with two 6 m spans and a 0.3 × 0.5 m^2 cross-section was considered, as represented in Fig. 15. Two steels with the same yield strength but different ductility classes were used, Class A ($f_y = 550$ MPa, $f_t = 580$ MPa and $\varepsilon_u = 2.5\%$) and Class C ($f_y = 550$ MPa, $f_t = 635$ MPa e $\varepsilon_u = 7.5\%$), representing the minimum mechanical properties according to the Eurocode 2. In the beam design, a degree of moment redistribution η of 30% over the internal support was considered, and external supports were assumed as pinned connections. The damage (only pitting corrosion) was introduced considering stress–strain relation curves for steel similar to Fig. 3 but with some adjustments to consider the two types of steel.

In Fig. 16, the results of the ultimate load and ultimate deflection as a function of rebar damage is shown. Since the tensile strength of the two steels is different, it was expected that the ultimate load of the beams with steel Class C would be higher than that of the beams with steel Class A. In addition, it is observed that the ultimate load decreases much more quickly with corrosion in beams with steel class A than in beams with steel class C. Thus, two important conclusions can be drawn: i) structures with high ductile steel rebars will have longer durability, especially if corrosion is slow, which happens in most structures; and ii) structures with high ductile steel rebars will have a higher level of safety, particularly from the instant the corrosion occurs. Regarding the deformation, the ultimate deflection of beams with steel class C is much higher than for beams with steel class A, in this case, about twice as high. This is also a very important observation, particularly when the loading consists of imposed deformations.

In Fig. 17, the ultimate beam deformation and crack pattern for beams with 30% damage are shown. Beam with high ductile steel rebars (class C) presents much higher deformation, a higher number of cracks and much higher crack opening than beam with low ductile steel rebars (class A). That is why, especially when the damage is high, the rotation capacity is higher for beams with steel class C, which allows higher levels of real redistribution and small reductions in the loading capacity of continuous beams or slabs.

Comparing the results of isostatic beams (experimental and numerical) with hyperstatic beams (numerical) for 20% damage and assuming the use of high ductile steel rebars, as studied in this paper, some findings can be stated: i) regarding the ultimate deflection, which depends directly on the rotation capacity, the average reduction is about 50% in isostatic beams, while it was only about 20% in hyperstatic beams (this

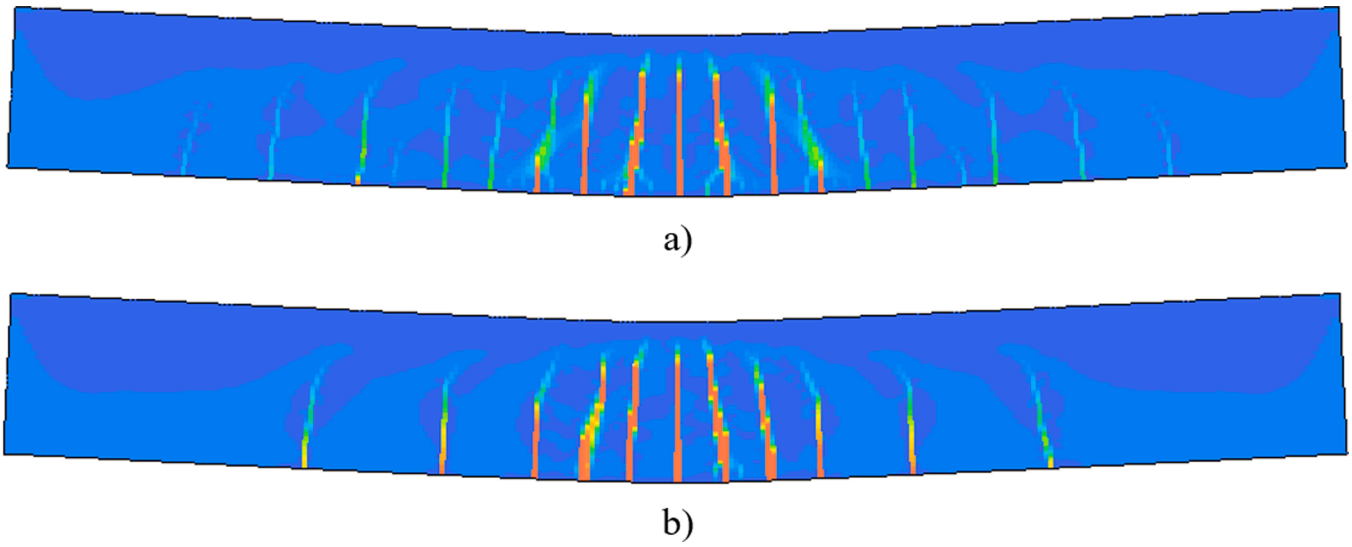

Fig. 13. Cracking patterns near the failure: a) pitting corrosion (V3), b) general and pitting corrosion (V5).

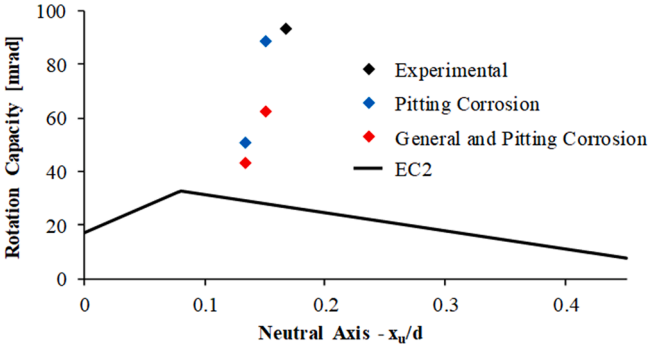

Fig. 14. Rotation capacity of damaged beams versus Eurocode 2 curve.

large difference occurs because, in hyperstatic beams, maximum deflection depends on midspan and support plastic behaviours, while in isostatic beams, it depends directly only on midspan plastic behaviour); ii) regarding the ultimate load, the average reduction was 12% for both isostatic and hyperstatic. These findings allow concluding that the corrosion of Special Ductility Tempcore rebars will affect the ultimate deflection of beams much more than their loading capacity, which is in agreement with results of other researchers [14–16] for other types of steel.

7. Conclusions

The corrosion of RC structures consumes many economic resources in developed countries to repair and reinforce these structures. Usually, corrosion not only diminishes the loading capacity but also the deformation capacity of the structures. When the original rebars have high ductility, the consequences of corrosion can be delayed because their effects are less severe. In this context, this paper aimed to assess the rotation capacity of corroded RC beams when using Special Ductility Tempcore rebars.

From the experimental campaign and numerical simulations developed, the following conclusions were drawn:

- The rotation capacity is seriously influenced by the corrosion. For 20% damage, the rotation capacity reduced about 50%. For 10% damage, the results were non-uniform. For pitting corrosion, the rotation capacity was not significantly changed; however, when general and pitting corrosion act simultaneously, the rotation capacity reduced about 33%.
- Although a high reduction was observed in rotation capacity for damage up to 20%, the values obtained in tests were higher than the Eurocode 2 and Model Code 2010 normalized curves.
- Especially for low levels of corrosion, the bond between concrete and rebars is important, influencing the rotation capacity.
- One way to increase the rotation capacity, in general, is by having a crack pattern with many cracks. To ensure it, some local damage should be done in the concrete at desired crack locations.

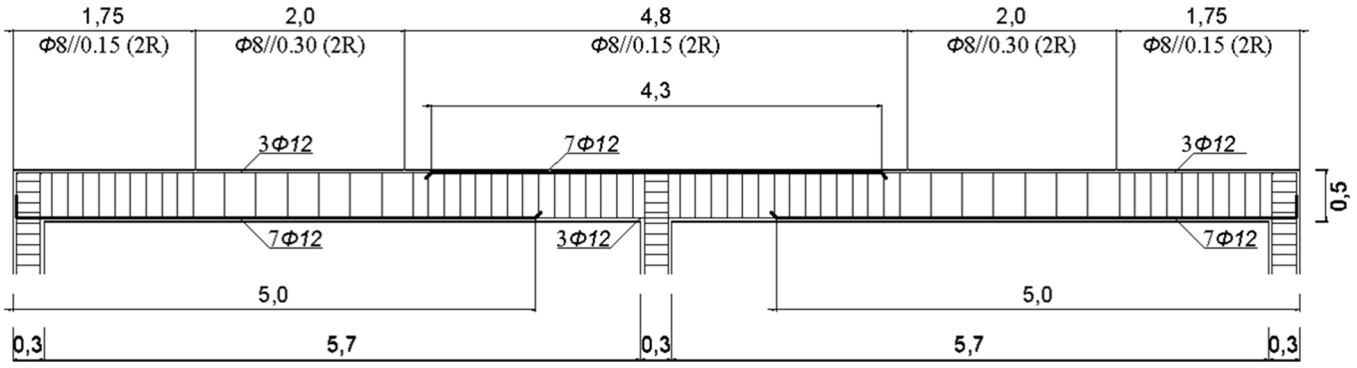

Fig. 15. Elevation of continuous beam analysed.

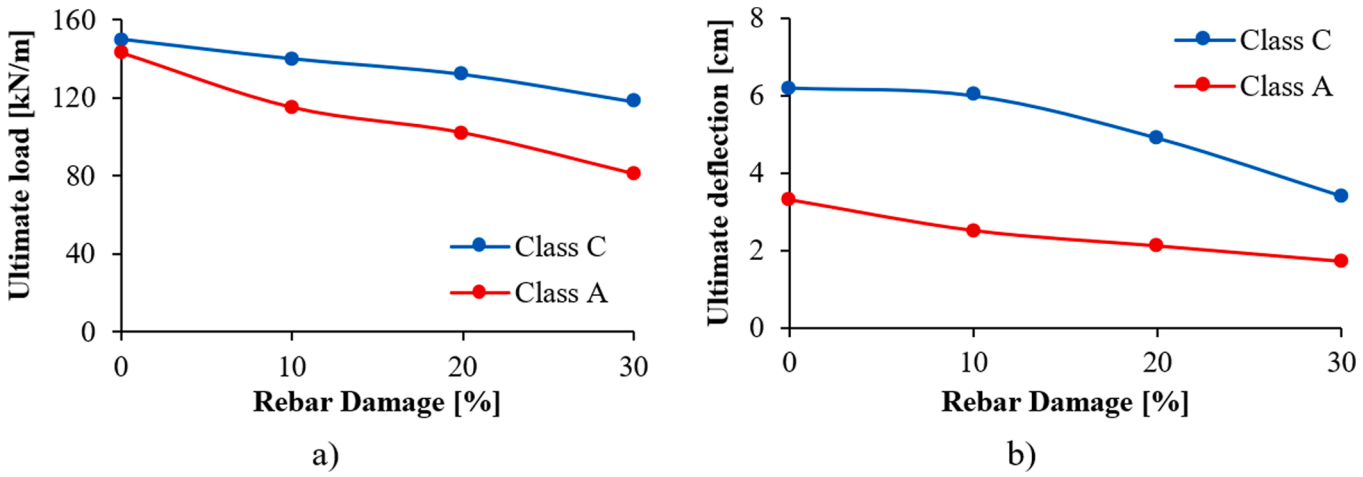

Fig. 16. Ultimate capacity of beam as a function of rebar damage: a) ultimate load, b) ultimate deflection.

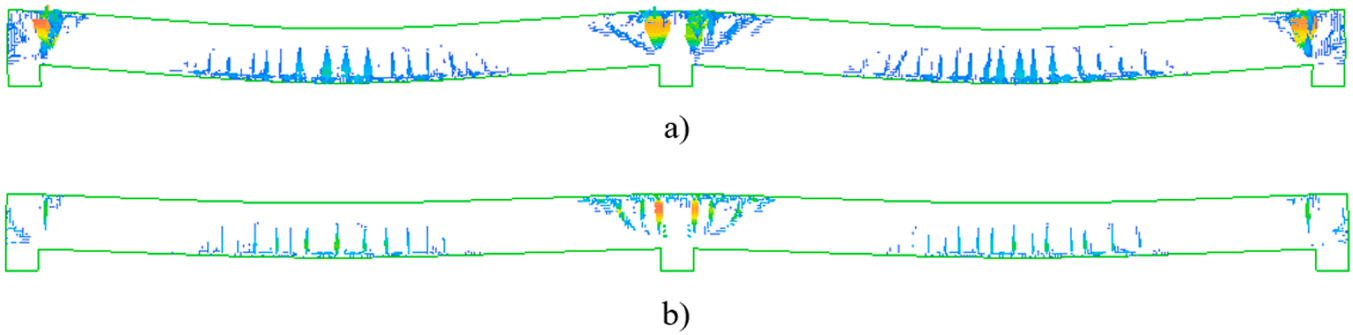

Fig. 17. Ultimate beam deformation (magnification factor: 5x) and crack pattern for 30% damage: a) Class C, b) Class A.

- Despite the high reduction observed in rotation capacity for 20% damage in the Special Ductility Tempcore rebars, the ultimate load of beams reduces only 12%.
- The numerical simulations can predict the rotation capacity correctly if a rigorous selection of the models for concrete in compression, rebar in tension and bond-slip is done.
- The bond element and bond-slip model proposed by the authors [47] tends to achieve better numerical results.
- Corrosion affects the ultimate deflection of isostatic beams much more than hyperstatic beams but for the ultimate load, the impact is similar and smaller.
- The ultimate load decreases much more quickly with corrosion in beams with steel class A than in beams with steel class C. The ultimate deflection of beams with steel class C is about two times higher than in the beams with steel class A for the same level of corrosion.

The results presented here could be useful at the time of deciding the best intervention for a reinforced concrete structure with corroded Special Ductility Tempcore rebars. Decisions like simple repair or full strengthen could be more sustained, which could allow many economic savings during the rehabilitation of our RC structures.

CRediT authorship contribution statement

José Santos: Conceptualization, Methodology, Software, Validation, Writing - original draft.

António Abel Henriques: Conceptualization, Resources, Writing - review & editing, Supervision, Funding acquisition.

Declaration of Competing Interest

The authors declare that they have no known competing financial interests or personal relationships that could have appeared to influence the work reported in this paper.

Acknowledgements

This work was financially supported by: Base Funding - UIDB/04708/2020 of the CONSTRUCT - Instituto de I&D em Estruturas e Construções - funded by national funds through the FCT/MCTES (PIDDAC).

References

[1] Šajna A, Legat A, Bjegović D, Kosec T, Oslaković IS, Serdar M, et al. Deliverable D11: Recommendations for the use of corrosion resistant reinforcement. FP6 Project Report: ARCHES 2009.
[2] Apostolopoulos CA, Papadakis VG. Consequences of steel corrosion on the ductility properties of reinforcement bar. Constr Build Mater 2008;22(12):2316–24. https://doi.org/10.1016/j.conbuildmat.2007.10.006.
[3] CEB. Ductility of reinforced concrete structures, Bulletin d'Information 242. Lausanne: Comité Euro-International du Béton; 1998.
[4] Santos José, Henriques António Abel. Span-to-depth ratio limits for RC continuous beams and slabs based on MC2010 and EC2 ductility and deflection requirements. Eng Struct 2021;228:111565. https://doi.org/10.1016/j.engstruct.2020.111565.
[5] Du YG, Clark LA, Chan AHC. Effect of corrosion on ductility of reinforcing bars. Mag Concr Res 2005;57(7):407–19. https://doi.org/10.1680/macr.2005.57.7.407.
[6] François Raoul, Khan Inamullah, Dang Vu Hiep. Impact of corrosion on mechanical properties of steel embedded in 27-year-old corroded reinforced concrete beams. Mater Struct 2013;46(6):899–910. https://doi.org/10.1617/s11527-012-9941-z.
[7] Tang F, Lin Z, Chen G, Yi W. Three-dimensional corrosion pit measurement and statistical mechanical degradation analysis of deformed steel bars subjected to accelerated corrosion. Constr Build Mater 2014;70:104–17. https://doi.org/10.1016/j.conbuildmat.2014.08.001.

[8] Zhu W, François R. Experimental investigation of the relationships between residual cross-section shapes and the ductility of corroded bars. Constr Build Mater 2014;69:335–45. https://doi.org/10.1016/j.conbuildmat.2014.07.059.
[9] Imperatore S, Rinaldi Z, Drago C. Degradation relationships for the mechanical properties of corroded steel rebars. Constr Build Mater 2017;148:219–30. https://doi.org/10.1016/j.conbuildmat.2017.04.209.
[10] Chen E, Berrocal Carlos G, Fernandez Ignasi, Löfgren Ingemar, Lundgren Karin. Assessment of the mechanical behaviour of reinforcement bars with localised pitting corrosion by Digital Image Correlation. Eng Struct 2020;219:110936. https://doi.org/10.1016/j.engstruct.2020.110936.
[11] Hawileh Rami A, Abdalla Jamil A, Al Tamimi Adil, Abdelrahman Khalid, Oudah Fadi. Behavior of Corroded Steel Reinforcing Bars Under Monotonic and Cyclic Loadings. Mech Adv Mater Struct 2011;18(3):218–24. https://doi.org/10.1080/15376494.2010.499023.
[12] Andisheh Kaveh, Scott Allan, Palermo Alessandro, Clucas Don. Influence of chloride corrosion on the effective mechanical properties of steel reinforcement. Struct Infrastruct Eng 2019;15(8):1036–48. https://doi.org/10.1080/15732479.2019.1594313.
[13] Castel A, François R, Arliguie G. Mechanical behaviour of corroded reinforced concrete beams—Part 1: Experimental study of corroded beams. Mater Struct 2000;33(9):539–44. https://doi.org/10.1007/BF02480533.
[14] Dang VH, François R. Influence of long-term corrosion in chloride environment on mechanical behaviour of RC beam. Eng Struct 2013;48:558–68. https://doi.org/10.1016/j.engstruct.2012.09.021.
[15] Dang VH, François R. Prediction of ductility factor of corroded reinforced concrete beams exposed to long term aging in chloride environment. Cem Concr Compos 2014;53:136–47. https://doi.org/10.1016/j.cemconcomp.2014.06.002.
[16] Almusallam Abdullah A, Al-Gahtani Ahmad S, Aziz Abdur Rauf, Dakhil Fahd H, Rasheeduzzafar. Effect of reinforcement corrosion on flexural behavior of concrete slabs. J Mater Civ Eng 1996;8(3):123–7. https://doi.org/10.1061/(ASCE)0899-1561(1996)8:3(123).
[17] Ou Y-C, Nguyen ND. Influences of location of reinforcement corrosion on seismic performance of corroded reinforced concrete beams. Eng Struct 2016;126:210–23. https://doi.org/10.1016/j.engstruct.2016.07.048.
[18] Yadav Divyashree, Kwatra Naveen, Agarwal Pankaj. Post-yield deformation parameters of reinforced concrete beam with corroded reinforcement. Structural Concrete 2019;20(1):318–29. https://doi.org/10.1002/suco.2019.20.issue-110.1002/suco.201800037.
[19] Ye H, Fu C, Jin N, Jin X. Performance of reinforced concrete beams corroded under sustained service loads: A comparative study of two accelerated corrosion techniques. Constr Build Mater 2018;162:286–97. https://doi.org/10.1016/j.conbuildmat.2017.10.108.
[20] Dong J, Zhao Y, Wang K, Jin W. Crack propagation and flexural behaviour of RC beams under simultaneous sustained loading and steel corrosion. Constr Build Mater 2017;151:208–19. https://doi.org/10.1016/j.conbuildmat.2017.05.193.
[21] Azad AK, Ahmad S, Al-Gohi BHA. Flexural strength of corroded reinforced concrete beams. Mag Concr Res 2010;62(6):405–14. https://doi.org/10.1680/macr.2010.62.6.405.
[22] Yu L, François R, Dang VH, L'Hostis V, Gagné R. Structural performance of RC beams damaged by natural corrosion under sustained loading in a chloride environment. Eng Struct 2015;96:30–40. https://doi.org/10.1016/j.engstruct.2015.04.001.
[23] Hansapinyo Chayanon, Vimonsatit Vanissorn, Matsushima Manabu, Limkatanyu Suchart. Critical amount of corrosion and failure behavior of flexural reinforced concrete beams. Constr Build Mater 2021;270:121448. https://doi.org/10.1016/j.conbuildmat.2020.121448.
[24] Du Y, Cullen M, Li C. Structural performance of RC beams under simultaneous loading and reinforcement corrosion. Constr Build Mater 2013;38:472–81. https://doi.org/10.1016/j.conbuildmat.2012.08.010.
[25] Liu Y, Jiang N, Deng Y, Ma Y, Zhang H, Li M. Flexural experiment and stiffness investigation of reinforced concrete beam under chloride penetration and sustained loading. Constr Build Mater 2016;117:302–10. https://doi.org/10.1016/j.conbuildmat.2016.04.110.
[26] Ma Yafei, Guo Zhongzhao, Wang Lei, Zhang Jianren. Probabilistic Life Prediction for Reinforced Concrete Structures Subjected to Seasonal Corrosion-Fatigue Damage. J Struct Eng 2020;146(7):04020117. https://doi.org/10.1061/(ASCE)ST.1943-541X.0002666.
[27] Guo Zhongzhao, Ma Yafei, Wang Lei, Zhang Xuhui, Zhang Jianren, Hutchinson Cody, et al. Crack Propagation-Based Fatigue Life Prediction of Corroded RC Beams Considering Bond Degradation. J Bridge Eng 2020;25(8):04020048. https://doi.org/10.1061/(ASCE)BE.1943-5592.0001592.
[28] Ma Yafei, Peng Anyin, Su Xiaochao, Wang Lei, Zhang Jianren. Modeling Constitutive Relationship of Steel Bar Removed from Corroded PC Beams after Fatigue Considering Spatial Location Effect. J Mater Civ Eng 2021;33(4):04021019. https://doi.org/10.1061/(ASCE)MT.1943-5533.0003644.
[29] Lundgren K. Effect of corrosion on the bond between steel and concrete: an overview. Mag Concr Res 2007;59(6):447–61. https://doi.org/10.1680/macr.2007.59.6.447.
[30] Irina Sæther BS. FEM simulations of reinforced concrete beams attacked by corrosion. ACI Structural Journal; 109:15-31.
[31] Biondini Fabio, Vergani Matteo. Deteriorating beam finite element for nonlinear analysis of concrete structures under corrosion. Struct Infrastruct Eng 2015;11(4):519–32. https://doi.org/10.1080/15732479.2014.951863.
[32] Hanjari KZ, Kettil P, Lundgren K. Analysis of mechanical behavior of corroded reinforced concrete structures. ACI Struct J 2011;108:532–41. https://doi.org/10.14359/51683210.
[33] Stewart Mark G. Mechanical behaviour of pitting corrosion of flexural and shear reinforcement and its effect on structural reliability of corroding RC beams. Struct Saf 2009;31(1):19–30. https://doi.org/10.1016/j.strusafe.2007.12.001.
[34] Kanchana Devi A, Ramajaneyulu K, Sundarkumar S, Ramesh G, Bharat Kumar BH, Krishna Moorthy TS. Ultimate Load Behaviour of Reinforced Concrete Beam with Corroded Reinforcement. Journal of The Institution of Engineers (India): Series A 2017;98(4):525–32. https://doi.org/10.1007/s40030-017-0239-6.
[35] Kallias AN, Imran Rafiq M. Performance assessment of corroding RC beams using response surface methodology. Eng Struct 2013;49:671–85. https://doi.org/10.1016/j.engstruct.2012.11.015.
[36] Lopes Sérgio M, do Carmo Ricardo NF. Deformable strut and tie model for the calculation of the plastic rotation capacity. Comput Struct 2006;84(31-32):2174–83. https://doi.org/10.1016/j.compstruc.2006.08.028.
[37] Haskett Matthew, Oehlers Deric John, Mohamed Ali MS, Wu Chengqing. Rigid body moment-rotation mechanism for reinforced concrete beam hinges. Eng Struct 2009;31(5):1032–41. https://doi.org/10.1016/j.engstruct.2008.12.016.
[38] Zhou KJH, Ho JCM, Su RKL. Normalised rotation capacity for deformability evaluation of high-performance concrete beams. Earthquake and Structures 2010;1(3):269–87.
[39] Arcer TC. Characteristic Stress-Strain Curves for ARCER Mark Special Ductility Weldable Steel. Madrid: ARCER; 2003.
[40] fib. Bulletin 55 - Model Code 2010 - First complete draft, Volume 1. Lausanne, Switzerland: International Federation for Structural Concrete (fib); 2010.
[41] EN 1992-1-1. Eurocode 2: Design of concrete structures - Part 1-1: General rules and rules for buildings. Brussels, Belgium: European Committee for Standardization; 2004.
[42] Santos J, Henriques AA. Strength and Ductility of Damaged Tempcore Rebars. Procedia Eng 2015;114:800–7. https://doi.org/10.1016/j.proeng.2015.08.029.
[43] Liu Xiguang, Zhang Weiping, Gu Xianglin, Ye Zhiwen. Probability distribution model of stress impact factor for corrosion pits of high-strength prestressing wires. Eng Struct 2021;230:111686. https://doi.org/10.1016/j.engstruct.2020.111686.
[44] Manie J, Kikstra WP. DIANA-9.42 User's Manual - Material Library. TNO DIANA BV, Delft 2010.
[45] Santos J, Henriques AA. Modelling of Reinforced Concrete Beams With Low Tensile Reinforcement Ratio. CoRAN 2011 – International Conference on Recent Advances in Nonlinear Models – Structural Concrete Applications. Coimbra, Portugal2011.
[46] Santos J, Henriques AA. FE modelling of bond-slip response including steel strains. Bond in Concrete 2012: Bond, Anchorage, Detailing (4th International Symposium). Brescia, Italy2012.
[47] Santos J, Henriques AA. New finite element to model bond–slip with steel strain effect for the analysis of reinforced concrete structures. Eng Struct 2015;86:72–83. https://doi.org/10.1016/j.engstruct.2014.12.036.
[48] Rots JG, Blaauwendraad J. Crack models for concrete: discrete or smeared? Fixed, multi-directional or rotating? Heron 1989;34:3–59.
[49] fib. Bulletin 10 - Bond of Reinforcement in concrete. Lausanne, Switzerland: International Federation for Structural Concrete (fib); 2000.
[50] Chung Lan, Jay Kim Jang-Ho, Yi Seong-Tae. Bond strength prediction for reinforced concrete members with highly corroded reinforcing bars. Cem Concr Compos 2008;30(7):603–11. https://doi.org/10.1016/j.cemconcomp.2008.03.006.
[51] Ouglova Anna, Berthaud Yves, Foct François, François Marc, Ragueneau Frédéric, Petre-Lazar Ilie. The influence of corrosion on bond properties between concrete and reinforcement in concrete structures. Materials and Structures/Materiaux et Constructions 2008;41(5):969–80. https://doi.org/10.1617/s11527-007-9298-x.
[52] Chung Lou, Najm Husam, Balaguru Perumalsamy. Flexural behavior of concrete slabs with corroded bars. Cem Concr Compos 2008;30(3):184–93. https://doi.org/10.1016/j.cemconcomp.2007.08.005.